EMBO reports

scientific report

Mutations in the relay loop region result in dominant-negative inhibition of myosin II function in *Dictyostelium*

Georgios Tsiavaliaris[1,+], Setsuko Fujita-Becker[1], Renu Batra[1,†], Dmitrii I. Levitsky[2], F. Jon Kull[1,‡], Michael A. Geeves[3] & Dietmar J. Manstein[1,+,‡]

[1]Max-Planck-Institut für medizinische Forschung, Jahnstrasse 29, D-69120 Heidelberg, Germany, [2]A.N.Bach Institute of Biochemistry, Russian Academy of Science, Moscow 119071, Russia and [3]Department of Biosciences, University of Kent, Canterbury, Kent CT2 7NJ, UK

Received July 8, 2002; revised August 29, 2002; accepted September 4, 2002

Dominant-negative inhibition is a powerful genetic tool for the characterization of gene function *in vivo*, based on the specific impairment of a gene product by the coexpression of a mutant version of the same gene product. We describe the detailed characterization of two myosin constructs containing either point mutations F487A or F506G in the relay region. *Dictyostelium* cells transformed with F487A or F506G myosin are unable to undergo processes that require myosin II function, including fruiting-body formation, normal cytokinesis and growth in suspension. Our results show that the dominant-negative inhibition of myosin function is caused by disruption of the communication between active site and lever arm, which blocks motor activity completely, and perturbation of the communication between active site and actin-binding site, leading to an ~100-fold increase in the mutants' affinity for actin in the presence of ATP.

INTRODUCTION

The N-terminal, globular domain of myosin interacts with actin filaments, producing force and movement in an ATP-dependent fashion. High-resolution structural data of this domain show the myosin motor to be composed of a central core, which contains the nucleotide-binding site and is structurally related to G-proteins (Vale, 1996). Extensions to this central core form the actin-binding site and the relay, converter and lever arm regions. A major function of these three regions is the amplification of the small conformational changes occurring at the active site to the large changes required for the movement of actin filaments (Geeves and Holmes, 1999).

The central core structure consists of seven β-strands and six α-helices and contains a group of conserved sequence motifs, termed switch-1 and switch-2, that contact the nucleotide at the rear of the nucleotide-binding pocket and act as γ-phosphate sensors. Switch-1 and switch-2 move towards each other when ATP is bound and move away from each other when ADP occupies the binding pocket, with switch-2 undergoing a large conformational change, whereas switch-1 contributes only minor conformational changes. The resulting conformational states are referred to as *closed* (ATP bound) and *open* (ADP or no nucleotide bound). Outside the nucleotide-binding pocket, conformational changes during the transition from *open* to *closed* are limited to a subset of regions and nearly all of them take place by rigid-body rotations of secondary and tertiary structure elements (Rayment *et al.*, 1993; Dominguez *et al.*, 1998; Kollmar *et al.*, 2002). Therefore, the core and its extensions can be regarded as communicating functional units with substantial movement occurring in only a few residues. Some of the largest rotations in the angles of Φ and Ψ bonds are observed in the relay region, which serves as a central communication hub (Geeves and Holmes, 1999). Closure of the γ-phosphate-binding site results in the formation of a sharp kink in the switch-2 helix and a 60° twisting near its end, which is part of the relay region (Figure 1). This motion affects the angular position of the

+Present address: Institut für Biophysikalische Chemie, Medizinische Hochschule Hannover, Carl-Neuberg-Straße 1, Hannover, Germany.
†Present address: Institut für Biologische Informationsverarbeitung, Forschungzentrum Jülich, 52425 Jülich, Germany.
‡Present address: Dartmouth College, 6128 Burke Laboratory, Hanover, NH 03755, USA.
‡Corresponding author. Medizinische Hochschule Hannover, Institute for Biophysical Chemistry, OE 4350, Carl-Neuberg-Straße 1, D-30623 Hannover, Germany; Tel: +49 511 532 3700; Fax: +49 511 532 5966; E-mail: manstein@bpc.mh-hannover.de

lever arm and the actin-binding site. Communication to the actin-binding site follows the path of the polypeptide chain, whereas a cluster of highly conserved hydrophobic residues mediates the coordinated movement of the relay region and converter region in response to conformational changes in the nucleotide-binding site. Hydrophobic interactions mediated by these residues are critical for at least two functions: residues Y494, I499, W501, F692 and F745 link the end of the relay helix to the converter domain, with the effect that both move as a rigid unit; residues N483, F487, F506, L508 and I687 appear to be important for stabilizing the bent form of the relay helix, which is present in the hydrolytically competent *closed* state of myosin (Kollmar *et al.*, 2002). Here, we examine myosin motor domain and full-length constructs containing point mutations leading to the substitution of either residue F487 or F506. Constructs with point mutations F487A, F506A and F506G were generated. However, as all three constructs showed similar or identical properties, we only report results obtained with F506G and selected results obtained with F487A.

RESULTS AND DISCUSSION

In the *Dictyostelium* system, the functionality of a mutant myosin can be easily assessed *in vivo*. Normal cytokinesis, growth in suspension culture, capping of cell surface receptors and sporogenesis are processes that require a functional myosin II in *Dictyostelium* (De Lozanne and Spudich, 1987). Complementation of myosin null cells (Manstein *et al.*, 1989) with F487A- and F506G-myosin did not restore the functional defects, indicating that the point mutations disrupt myosin function. Additionally, we found that expression of the mutant myosins interferes with normal myosin II function in a dominant-negative way. Wild-type cells transformed with F487A- or F506G-myosin were unable to undergo fruiting-body formation and cytokinesis and failed to grow in suspension (Figure 2). Partial impairment of myosin II function in *Dictyostelium* has been reported previously for the coexpression of the tail portion of myosin II, which leads to the formation of single-headed myosin II and interferes with cytokinesis but not sporogenesis (Burns *et al.*, 1995). Dominant mutations have been described for the *Caenorhabditis elegans* body wall myosin UNC-54 (Bejsovec and Anderson, 1990) however, mutations of the equivalent residues in the ATP and actin-binding sites of *Dictyostelium* myosin II have no dominant-negative effect.

To determine the cause of the dominant-negative effect of the F487A or F506G full-length constructs, we produced the point mutations separately in the myosin motor domain construct M761-2R (Anson *et al.*, 1996). M761-2R consists of the first 761 amino acids of the motor domain of *Dictyostelium discoideum* myosin II fused to two α-actinin repeats in place of the native light chain binding domain. M761-2R displays S1-like kinetic and motile properties (Kurzawa *et al.*, 1997; Kliche *et al.*, 2001). The mutant constructs will be referred to as F487A-2R and F506G-2R.

Differential scanning calorimetry (DSC) was used to examine whether the elimination of a single phenylalanine residue from the cluster of highly conserved hydrophobic residues is sufficient to disrupt the coordinated movement of the relay and converter regions. DSC is sensitive to conformational changes that occur in the globular motor portion of myosin following strong binding

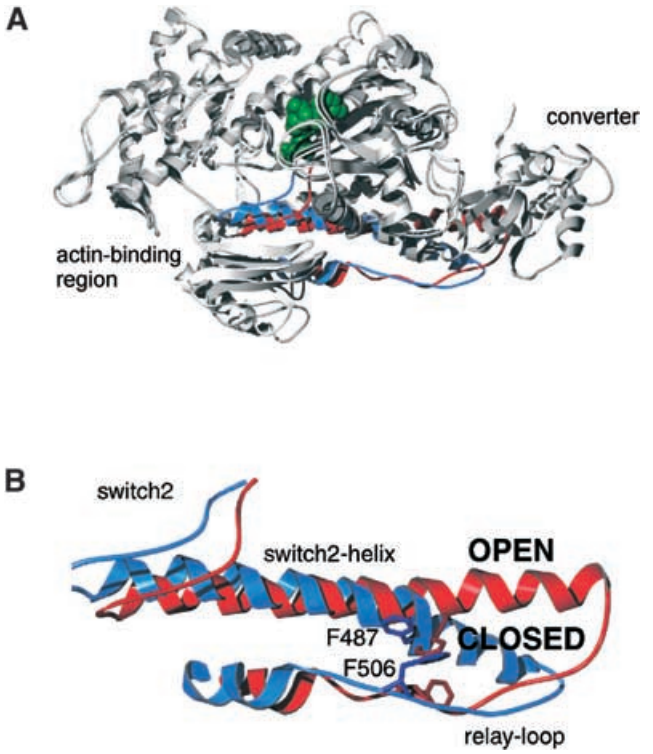

Fig. 1. Superposition of myosin motor domain structures in the *open* and *closed* states. (**A**) The converter follows the movement of the switch-2 helix during the transition from the *open* to the *closed* state. (**B**) Close-up view of the switch-2 and relay regions. Changes in the orientation of the relay-loop and bending of the switch-2 helix are observed. The figure was produced with the Swiss-PDB Viewer (Guex and Peitsch, 1997).

to F-actin or the formation of stable ternary complexes with ADP and P_i analogues (Levitsky *et al.*, 1998; Ponomarev *et al.*, 2000). In the case of wild-type myosin, discrete increases in the thermal stability of the protein are observed, which reflect the transitions between *open* in the absence of nucleotide, *open* in the presence of ADP, *closed* in the presence of ATP and ADP-P_i analogues and *open* in the presence of ADP and F-actin (Figure 3). The difference between the maximum of the thermal transitions for actin-free and actin-bound F506G-2R (ΔT_m = 4.7°C) is 20% smaller than that observed with a wild-type construct (ΔT_m = 6.0°C) (Ponomarev *et al.*, 2000), indicating differences in the coupling between nucleotide- and actin-binding sites. Furthermore, the calorimetric traces for the thermally induced unfolding of F506G-2R complexed with ADP, ADP-V_i, ADP-BeF_3 or ADP-AlF_4 show similar shifts of the maximum of the thermal transition (T_m) relative to the T_m value observed for nucleotide-free F506G-2R (Figure 3). These results are in good agreement with a model where nucleotide binding leads to an ~4°C stabilization of the motor domain. However, additional increases in T_m, as observed for the wild-type protein upon formation of stable ternary complexes with ADP and P_i analogues, require closure of the P_i binding pocket and the concerted movement of relay region and converter.

Additional support for the disruption of the coordinated movement of relay region and converter by the point mutations comes from the loss of the characteristic enhancement in tryptophan

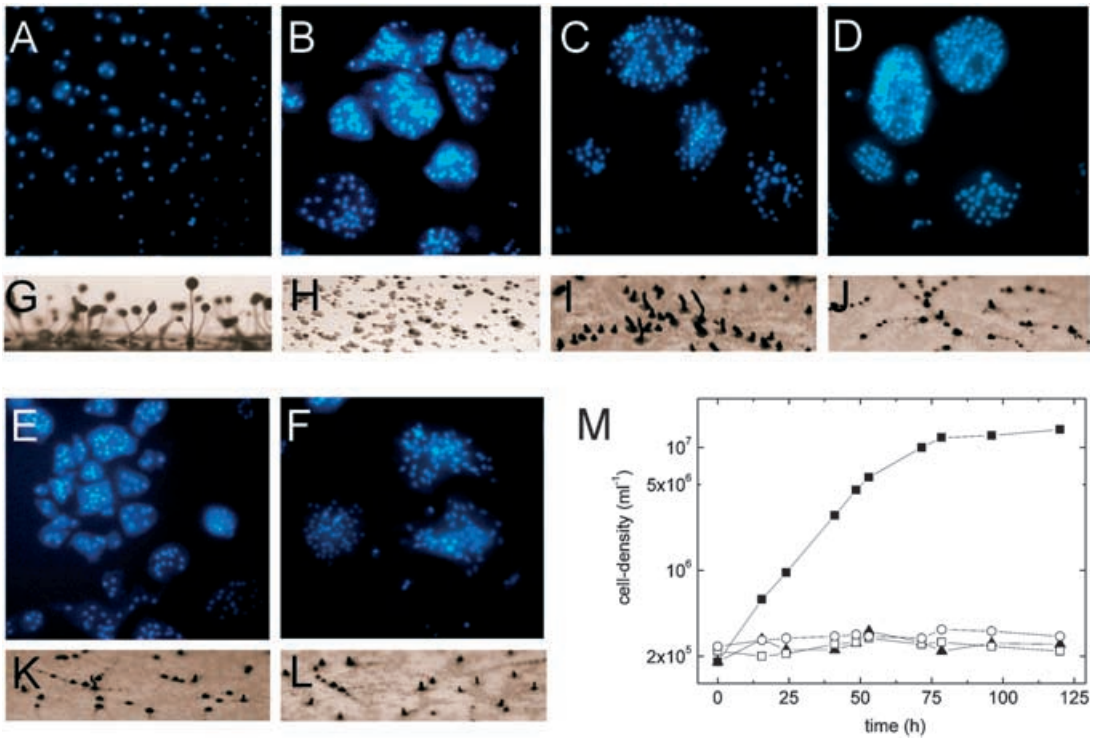

Fig. 2. Dominant-negative effect of mutations F487A and F506G. Normal cytokinesis, fruiting body formation and growth in suspension are myosin II-dependent processes. (**A**) *Dictyostelium* wild-type cells stained with the nuclear dye DAPI; (**B–F**) staining with DAPI shows that myosin II-depleted cells and cells producing F487A-FL or F506G-FL become large and multinucleate. (**H**) Myosin II-null cells aggregate but fail to form fruiting bodies consisting of a stalk and spore head; (**I–L**) cells producing F487A-FL or F506G-FL fail to form fruiting bodies. (A and G) Wild-type; (B and H) myosin II-null cells; (C and I) wild-type cells producing F506G-FL; (D and J) myosin II-null cells producing F506G-FL; (E and K) wild-type cells producing F487A-FL; (F and L) myosin null cells producing F487A-FL. (M) Cell growth in suspension culture. Wild-type cells grow with a doubling time of 8 h (filled squares). Similar to myosin II-null cells (open circles), wild-type cells producing F506G myosins (filled triangles) or F487A myosin (open squares) are not able to grow in suspension culture.

fluorescence, which has been widely exploited for the kinetic characterization of myosins. Crystal structures show Trp501 or the equivalent residue in vertebrate smooth muscle myosin to change from a more exposed environment in *open* to a less exposed, hydrophobic environment in *closed* structures. In agreement with these changes in microenvironment, ATP binding to *Dictyostelium* myosin II, which favours the *closed* state, leads to a 25% increase in the intrinsic fluorescence of Trp501 (Batra and Manstein, 1999). In contrast, addition of excess ATP to F506G-2R and F487A-2R results in a 4–6% decrease in intrinsic fluorescence (data not shown).

Disruption of the coordinated movement of the relay and converter regions is predicted to greatly reduce or abolish motor activity. F506G-2R and F487A-2R did not move actin filaments in *in vitro* motility assays (Kron and Spudich, 1986). Mixing assays, allowing an estimate of the duration for which the mutant construct is attached to actin during a catalytic turnover (Giese and Spudich, 1997), were used to measure the inhibition of rabbit HMM motility by F506G-2R. At a one-to-one ratio of rabbit HMM to F506G-2R, we observed a >3-fold reduction in velocity, whereas a one-to-one mixture of rabbit HMM with the corresponding wild-type construct reduced the velocity of rabbit HMM by only 35%. Higher ratios of F506G completely inhibited velocity (data not shown). These results suggest that the mutant constructs do not only disrupt the communication between the nucleotide-binding site and the lever arm but that the mutations affect a kinetic step resulting in prolonged actin attachment.

Stopped-flow analysis of F487A-2R and F506G-2R showed that the second-order rate constants for ATP binding (K_1k_{+2}) and ADP binding (k_6/K_7), *rigor* binding to actin ($\mathbf{k_{+A}}$, $\mathbf{k_{-A}}$) and coupling between actin binding and ADP affinity ($\mathbf{K_{AD}}/K_D$) are not affected by the mutations (Tables I and II). In contrast, steady-state measurements revealed large differences in the interaction with actin and ATP between the mutant and wild-type constructs. F487A-2R and F506G-2R exhibit 2- to 5-fold elevated basal ATPase activity (0.12 and 0.3 s^{-1}), reduced k_{cat} values of ~0.4 s^{-1}, and a 50- (F506G) to 270-fold (F487A) increased actin affinity in the presence of ATP (K_{app}). A value for the K_{app} of 135 μM was determined for M761-2R. As the small differences between k_{basal} and k_{cat} make a more exact determination of K_{app} difficult, we used single turnover kinetics with mantATP as substrate to confirm the increased actin affinity of the mutant constructs in the presence of nucleotide (Figure 4). Three phases could be distinguished following mixing of mantATP and M761-2R: (1) an initial fast rise of the fluorescence signal, (2) a plateau phase and (3) a slow decrease of the fluorescence signal, where phases 1 and 3 reflect the binding of mantATP and dissociation of mantADP, and phase 2 monitors the duration of the hydrolysis reaction. Addition of increasing amounts of F-actin led to a linear acceleration of the

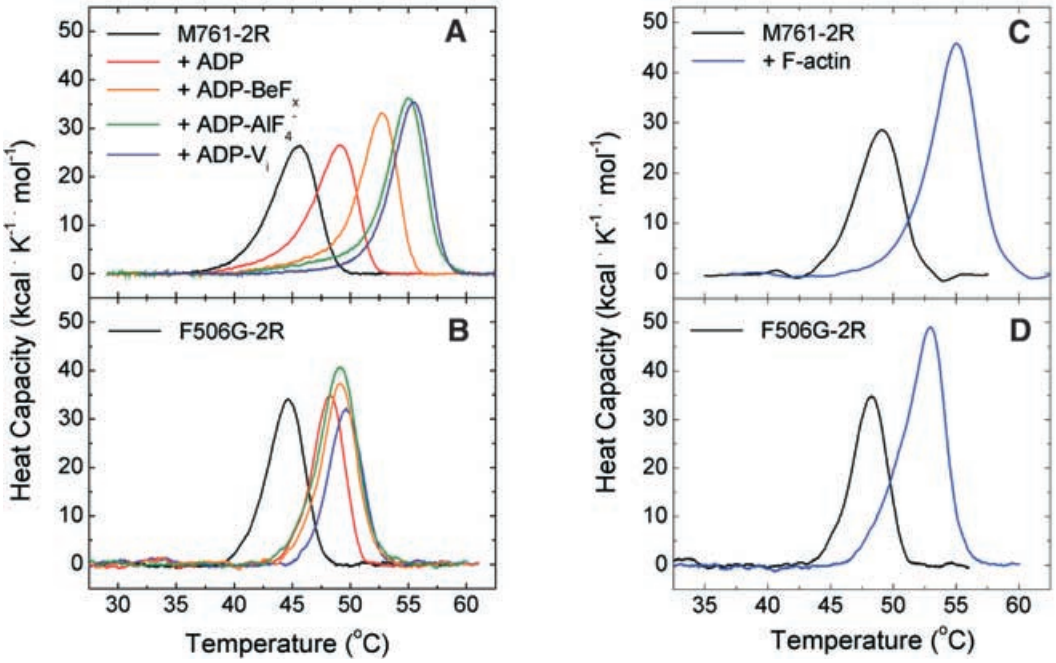

Fig. 3. Ligand-dependent thermal stabilization of myosin motor domain constructs. DSC was used to examine nucleotide dependent changes in thermal unfolding. (**A**) M761-2R shows an ~5°C shift of the maximum of the thermal transition following binding of ADP and additional thermal stabilization upon formation of ternary complexes with ADP and P_i analogues (V_i, BeF_x, AlF_4). (**B**) F506G-2R shows a similar shift in T_m in the presence of ADP. In contrast, ternary complexes of F506G-2R with ADP and P_i analogues produce only minor increases in T_m. (**C**) In the presence of ADP, F-actin binding to M761-2R leads to a 6.0°C shift in T_m. (**D**) F506G-2R shows a 4.7°C shift in T_m after addition of F-actin.

rate of mantADP dissociation. When the same experiment was repeated with F506G-2R, only two phases could be distinguished in the absence of actin; a fast rise in fluorescence, followed by a plateau with no signal decrease occurring during the next 1000 s. Quenched-flow experiments revealed that the nucleotide was hydrolysed with a rate of 0.06 s^{-1} (data not shown), indicating that the plateau was caused by slow dissociation of the hydrolysis products and not by a limiting hydrolysis rate. Addition of actin led to the reappearance of phase 3, indicating acceleration of the rate of mantADP dissociation. The increase in the k_{obs} of phase 3 with increasing actin concentration is a measure of the efficiency with which actin binds to the M·mantATP or M·mantADP-P_i complex. For F506G-2R, the increase in k_{obs} with increasing actin concentration could be fitted to a hyperbola with $K_{0.5}$ = 1 μM (Figure 4B). This value is similar to that determined for the K_{app} of F506G-2R.

Our results confirm the importance of the relay loop region as a communication zone, mediating conformational information between the converter domain, the nucleotide-binding site and the actin-binding site. They demonstrate the importance of a conserved hydrophobic cluster for the efficient conformational coupling between the active site and the lever arm and show that changes in the relay loop perturb communication between the active site and the actin-binding site. The high degree of conservation in this region suggests that the generation of myosin constructs containing mutations equivalent to F506G, F506A and F487A will provide a powerful tool to dissect the functional properties of myosins from all classes *in vivo* and in more complex systems than *Dictyostelium*.

METHODS

Plasmid construction. Enzymes were obtained from MBI-Fermentas (St Leon-Roth, Germany) and New England Biolabs (Frankfurt, Germany). *Escherichia coli* strain XL1Blue (Stratagene, Heidelberg, Germany) was used for amplification of plasmids. The expression vectors used for the production of mutant myosin constructs were based on the extrachromosomal vector pDXA-3H (Manstein *et al.*, 1995). M761-2R and full-length myosin constructs were generated using plasmids pDH12 (Kurzawa *et al.*, 1997) and pDH (Furch *et al.*, 1999), respectively. All DNA constructs were confirmed by sequencing.

Protein production and purification. Plasmids were transformed into Orf and mhcA$^-$ cells by electroporation. Transformants were grown at 21°C in HL-5C medium and selected in the presence of 10 μg/ml G418 and 100 U/ml penicillin-streptomycin. Screening for the production of the recombinant myosins and protein purification was performed as described previously (Manstein and Hunt, 1995). Rabbit skeletal muscle actin was purified as described by Lehrer and Kewar (1972) and pyrene-labelled as described by Criddle *et al.* (1985). Rabbit HMM was prepared as described by Margossian and Lowey (1982).

***Dictyostelium* manipulation.** Synchronous morphological differentiation was induced by starvation on MMC agar (20 mM MES, 2 mM $MgCl_2$, 0.2 mM $CaCl_2$, and 2% w/v Bacto agar) adjusted to pH 6.8. Structures from various stages of development were visualized using an Olympus B061 microscope and a Sony SSC-M370CE video camera. A Hamamatsu Argus-20 was used for contrast enhancement and transfer of images to a

Table I. Transient kinetic analysis of mutants and wild-type myosin

Nucleotide	Rate constant	M761–2R	F506G-2R	F487A-2R
ATP	K_1k_{+2} ($M^{-1}s^{-1}$)	$7.0 \pm (0.4) \times 10^5$	$6.7 \pm (0.2) \times 10^5$	$6.2 \pm (0.1) \times 10^5$
	$k_{+3} + k_{-3}$ (s^{-1})	28 ± (4)	–	–
	k_{+2} (s^{-1})	–	>500	>250
mantATP	K_1k_{+2} ($M^{-1}s^{-1}$)	$8.1 \pm (0.2) \times 10^5$	$5.3 \pm (0.1) \times 10^5$	$9.1 \pm (0.4) \times 10^5$
ADP	k_6/K_7 ($M^{-1}s^{-1}$)	no signal	$9 \pm (0.1) \times 10^5$	$22 \pm (0.7) \times 10^5$
	K_D (μM)	7.1 ± (0.5)	1.6 ± (0.2)	3.1 ± (0.4)
mantADP	k_{+D} ($M^{-1}s^{-1}$)	$4.8 \pm (0.1) \times 10^5$	$5.0 \pm (0.3) \times 10^5$	$13.2 \pm (1.1) \times 10^5$
	k_{-D} (s^{-1})	1.34 ± (0.1)	0.34 ± (0.04)	0.8 ± (0.1)
	K_D (μM)	2.8 ± (0.2)	0.68 ± (0.1)	0.61 ± (0.1)

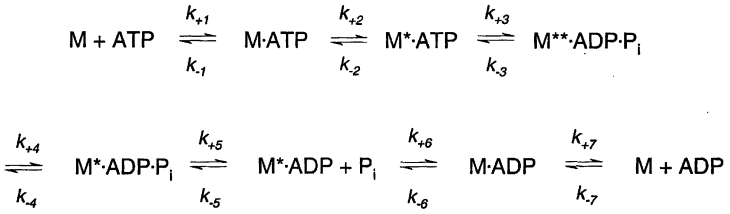

Binding and hydrolysis of ATP by myosin was analysed in terms of the seven-step model shown above (Bagshaw *et al.*, 1974).

Table II. Transient kinetic analysis of actin with mutants and wild-type myosin

Nucleotide	Rate constant	M761–2R	F506G-2R	F487A-2R
Nucleotide binding to actomyosin				
ATP	K_1k_{+2} ($M^{-1}s^{-1}$)	$5.7 \pm (0.4) \times 10^5$	$4.8 \pm (0.2) \times 10^5$	$3.7 \pm (0.2) \times 10^5$
	K_1 (s^{-1})	1000	500	400
	k_{+2} (s^{-1})	~500	>1000	>1000
ADP	K_{AD} (μM)	182 ± (28)	44 ± (6)	84 ± (9)
	k_{+AD} ($M^{-1}s^{-1}$)	$>0.5 \times 10^6$	$>0.5 \times 10^6$	$>0.2 \times 10^6$
	k_{-AD} (s^{-1})	>100	>20	>20
	K_{AD}/K_D	24 ± (3)	28 ± (4)	27 ± (3)
Actin binding to myosin				
	k_{+A} ($M^{-1}s^{-1}$)	$8.0 \pm (0.1) \times 10^5$	$2.7 \pm (0.3) \times 10^5$	$8.0 \pm (0.1) \times 10^5$
	k^-_A (ms^{-1})	2.5 ± (0.4)	1.6 ± (0.3)	5.0 ± (1)
	K_A (nM)	3.1 ± (0.5)	5.9 ± (0.7)	6.2 ± (0.8)
	K_{DA} (nM)	79.5 ± (14)	162 ± (23)	168 ± (29)
	k_{+DA} ($\mu M^{-1}s^{-1}$)	0.14 ± (0.01)	0.11 ± (0.01)	0.28 ± (0.02)
	k_{-DA} (s^{-1})	$11.1 \pm \times 10^{-3}$	$17.8 \pm \times 10^{-3}$	$47.0 \pm \times 10^{-3}$
	k_{-DA}/k_{-A}	4.4 ± 0.6	11.1 ± 1.3	9.4 ± 0.8

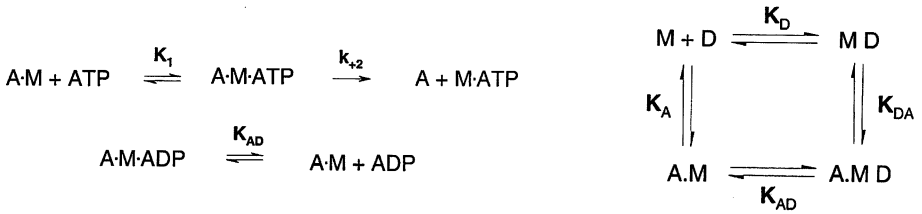

Actomyosin interactions were analysed in terms of the schemes shown above (Millar and Geeves, 1983; Siemankowski and White, 1984).

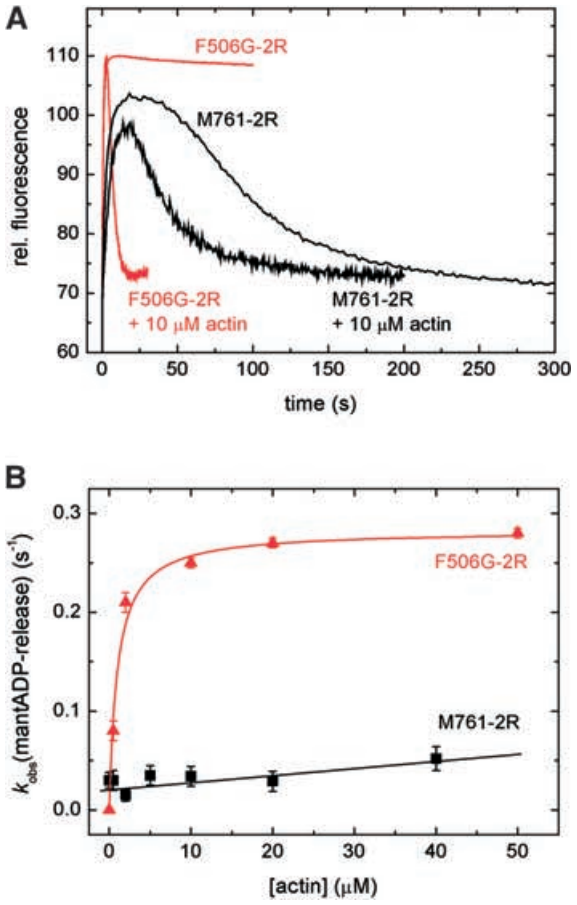

Fig. 4. Single turnover kinetics were used to measure the actin affinity of the mutant construct in the presence of mant-nucleotides. (**A**) Changes in fluorescence signal intensity following mixing of 2 μM M761-2R or F506G-2R with 1.75 μM mantATP in the presence and absence of F-actin. (**B**) The acceleration of mantADP release with increasing F-actin concentration could be described by a hyperbola with an apparent equilibrium dissociation constant $K_{0.5}$ = 1 μM. Addition of F-actin to M761-2R resulted in weaker and linear stimulation of mantADP release. The experiments shown were carried out in 20 mM MOPS, 100 mM KCl, 5 mM $MgCl_2$ at pH 7.0 and 20°C. In buffer containing only 25 mM KCl, the relationship between mantADP release and F-actin concentration for M761-2R could be described by a hyperbola with an apparent equilibrium dissociation constant $K_{0.5} \approx 150$ μM (data not shown).

Macintosh 9500. DAPI staining was performed as described previously (De Lozanne and Spudich, 1987).

Protein characterization. Fluorescence emission spectra were recorded at 20°C in a SLM 8000 fluorescence spectrophotometer. Transient kinetic and single turnover measurements were performed using a Hi-tech Scientific SF-61DX2 stopped-flow spectrophotometer as described previously (Furch *et al.*, 1999). All concentrations refer to the concentration of the reactants after mixing in the stopped-flow observation cell. Steady-state ATPase activities were determined at 25°C using a linked enzyme assay and analysed as described previously (Furch *et al.*, 1998). A notation is used that distinguishes between rate and equilibrium constants in the presence and absence of actin by using bold ($\mathbf{k_{+1}}$, $\mathbf{K_1}$) versus italic type (k_{+1}, K_1); subscript A and D refer to actin ($\mathbf{K_A}$) and ADP (K_D), respectively.

DSC experiments were performed on a DASM-4M differential scanning microcalorimeter (Institute for Biological Instrumentation, Puschchino, Russia) as described previously (Ponomarev *et al.*, 2000). Transition temperatures (T_m) were determined from the maximum of the temperature dependence of the molar heat capacity. Calorimetric enthalpies (ΔH_{cal}) were calculated from the area under the excess heat capacity curves.

In vitro motility was measured using standard sliding-filament assay methods at 30°C (Kron and Spudich, 1986; Anson *et al.*, 1996).

ACKNOWLEDGEMENTS

We thank S. Zimmermann for excellent technical assistance in the generation of expression vectors, M.L.W. Knetsch for help and stimulating discussions and M. Kollmar for contributing Figure 1, and K. C. Holmes for encouragement and continuous support. The work presented was supported by the Max-Planck-Society, Deutsche Forschungsgemeinschaft grants MA 1081/5-2 (to D.J.M.), Ku-1288/2-2 (to F.J.K.), GK388 (to G.T.), Wellcome Trust grant 055841 (to M.A.G.), and INTAS-RFBR Grant IR-97-577 (to D.I.L., D.J.M. and M.A.G.).

REFERENCES

Anson, M., Geeves, M.A., Kurzawa, S.E. and Manstein, D.J. (1996) Myosin motors with artificial lever arms. *EMBO J.*, **15**, 6069–6074.

Bagshaw, C.R., Eccleston, J.F., Eckstein, F., Goody, R.S., Gutfreund, H. and Trentham, D.R. (1974) The magnesium ion-dependent adenosine triphosphatase of myosin. Two-step processes of adenosine triphosphate association and adenosine diphosphate dissociation. *Biochem. J.*, **141**, 351–364.

Batra, R. and Manstein, D.J. (1999) Functional characterisation of *Dictyostelium* myosin II with conserved tryptophanyl residue 501 mutated to tyrosine. *Biol. Chem. Hoppe Seyler*, **380**, 1017–1023.

Bejsovec, A. and Anderson, P. (1990) Functions of the myosin ATP and actin binding sites are required for *C. elegans* thick filament assembly. *Cell*, **60**, 133–140.

Burns, C.G., Larochelle, D.A., Erickson, H., Reedy, M. and De Lozanne, A. (1995) Single-headed myosin II acts as a dominant negative mutation in *Dictyostelium*. *Proc. Natl Acad. Sci. USA*, **92**, 8244–8248.

Criddle, A.H., Geeves, M.A. and Jeffries, T. (1985) The use of actin labelled with *N*-(1-pyrenyl)iodoacetamide to study the interaction of actin with myosin subfragments and troponin/tropomyosin. *Biochem. J.*, **232**, 343–349.

De Lozanne, A. and Spudich, J.A. (1987) Disruption of the *Dictyostelium* myosin heavy chain gene by homologous recombination. *Science*, **236**, 1086–1091.

Dominguez, R., Freyzon, Y., Trybus, K.M. and Cohen, C. (1998) Crystal structure of a vertebrate smooth muscle myosin motor domain and its complex with the essential light chain: visualization of the pre-power stroke state. *Cell*, **94**, 559–571.

Furch, M., Geeves, M.A. and Manstein, D.J. (1998) Modulation of actin affinity and actomyosin adenosine triphosphatase by charge changes in the myosin motor domain. *Biochemistry*, **37**, 6317–6326.

Furch, M., FujitaBecker, S., Geeves, M.A., Holmes, K.C. and Manstein, D.J. (1999) Role of the salt-bridge between switch-1 and switch-2 of *Dictyostelium* myosin. *J. Mol. Biol.*, **290**, 797–809.

Geeves, M.A. and Holmes, K.C. (1999) Structural mechanism of muscle contraction. *Annu. Rev. Biochem.*, 687–728.

Giese, K.C. and Spudich, J.A. (1997) Phenotypically selected mutations in myosin's actin binding domain demonstrate intermolecular contacts important for motor function. *Biochemistry*, **36**, 8465–8473.

Guex, N. and Peitsch, M.C. (1997) SWISS-MODEL and the Swiss-PDBViewer: an environment for comparative protein modeling. *Electrophoresis*, **18**, 2714–2723.

Kliche, W., Fujita-Becker, S., Kollmar, M., Manstein, D.J. and Kull, F.J. (2001) Structure of a genetically engineered molecular motor. *EMBO J.*, **20**, 40–46.

Kollmar, M., Dürrwang, U., Kliche, W., Manstein, D.J. and Kull, F.J. (2002) Crystal structure of the motor domain of a class I myosin. *EMBO J.*, **21**, 2517–2525.

Kron, S.J. and Spudich, J.A. (1986) Fluorescent actin filaments move on myosin fixed to a glass surface. *Proc. Natl Acad. Sci. USA*, **83**, 6272–6276.

Kurzawa, S.E., Manstein, D.J. and Geeves, M.A. (1997) *Dictyostelium discoideum* myosin II: Characterization of functional myosin motor fragments. *Biochemistry*, **36**, 317–323.

Lehrer, S.S. and Kewar, G. (1972). Intrinsic fluorescence of actin. *Biochemistry*, **11**, 1211–1217.

Levitsky, D.I., Ponomarev, M.A., Geeves, M.A., Shnyrov, V.L. and Manstein, D.J. (1998) Differential scanning calorimetric study of the thermal unfolding of the motor domain fragments of *Dictyostelium discoideum* myosin II. *Eur. J. Biochem.*, **251**, 275–280.

Manstein, D.J. and Hunt, D.M. (1995) Overexpression of myosin motor domains in *Dictyostelium*: screening of transformants and purification of the affinity tagged protein. *J. Muscle Res. Cell Motil.*, **16**, 325–332.

Manstein, D.J., Titus, M.A., De Lozanne, A. and Spudich, J.A. (1989) Gene replacement in *Dictyostelium*—generation of myosin null mutants. *EMBO J.*, **8**, 923–932.

Manstein, D.J., Schuster, H.-P., Morandini, P. and Hunt, D.M. (1995) Cloning vectors for the production of proteins in *Dictyostelium discoideum*. *Gene*, **162**, 129–134.

Margossian, S.S. and Lowey, S. (1982) Preparation of myosin and its subfragments from rabbit skeletal muscle. *Methods Enzymol.*, **85**, 55–71.

Millar, N.C. and Geeves, M.A. (1983) The limiting rate of the ATP-mediated dissociation of actin from rabbit skeletal muscle myosin subfragment 1. *FEBS Lett.*, **160**, 141–148.

Ponomarev, M.A., Furch, M., Levitsky, D.I. and Manstein, D.J. (2000) Charge changes in loop 2 affect the thermal unfolding of the myosin motor domain bound to F-actin. *Biochemistry*, **39**, 4527–4532.

Rayment, I., Rypniewski, W.R., Schmidt-Bäse, K., Smith, R., Tomchick, D.R., Benning, M.M., Winkelmann, D.A., Wesenberg, G. and Holden, H.M. (1993) Three-dimensional structure of myosin subfragment-1: a molecular motor. *Science*, **261**, 50–58.

Siemankowski, R.F. and White, H.D. (1984) Kinetics of the interaction between actin, ADP, and cardiac myosin-S1. *J. Biol. Chem.*, **259**, 5045–5053.

Vale, R.D. (1996) Switches, latches, and amplifiers: common themes of G proteins and molecular motors. *J. Cell Biol.*, **135**, 291–302.

DOI: 10.1093/embo-reports/kvf214